CHEMISTRY
A EUROPEAN JOURNAL

DOI: 10.1002/chem.200600971

One-Electron versus Two-Electron Mechanisms in the Oxidative Addition Reactions of Chloroalkanes to Amido-Bridged Rhodium Complexes

Cristina Tejel,*[a] Miguel A. Ciriano,[a] José A. López,[a, b] Sonia Jiménez,[a] Marta Bordonaba,[a] and Luis A. Oro[a, b]

Dedicated to Professor Victor Riera on the occasion of his 70th birthday

Abstract: The compound *syn*-[{Rh(μ-NH{*p*-tolyl})(CN*t*Bu)$_2$}$_2$] (**1**) oxidatively adds C–Cl bonds of alkyl chlorides (RCl) and dichloromethane to each metal centre to give the cationic complexes *syn*-[{Rh(μ-NH{*p*-tolyl})(η^1-R)(CN*t*Bu)$_2$}$_2$(μ-Cl)]Cl and *anti*-[{Rh(μ-NH{*p*-tolyl})Cl(CN*t*Bu)$_2$}$_2$(μ-CH$_2$)]. Reaction of **1** with the chiral alkyl chloride (−)-(*S*)-ClCH(Me)CO$_2$Me (R*Cl) gave [{Rh(μ-NH{*p*-tolyl})(η^1-R*)(CN*t*Bu)$_2$}$_2$(μ-Cl)]Cl ([**3**]Cl) as an equimolecular mixture of the *meso* form (*R*,*S*)-[**3**]Cl-C_s and one enantiomer of the chiral form [**3**]Cl-C_2. This reaction, which takes place in two steps, was modeled step-by-step by reacting the mixed-ligand complex *syn*-[(cod)Rh(μ-NH{*p*-tolyl})$_2$Rh(CN*t*Bu)$_2$] (**4**) with R*Cl, as a replica of the first step, to give [(cod)Rh(μ-NH{*p*-tolyl})$_2$RhCl(η^1-R*)(CN*t*Bu)$_2$] (**5**) with racemization of the chiral carbon. Further treatment of **5** with CN*t*Bu to give the intermediate [(CN*t*Bu)$_2$Rh(μ-NH{*p*-tolyl})$_2$RhCl(η^1-R*)(CN*t*Bu)$_2$], followed by reaction with R*Cl reproduced the regioselectivity of the second step to give (*R*,*S*)-[**3**]Cl-C_s and [**3**]Cl-C_2 in a 1:1 molar ratio. Support for an S$_N$2 type of reaction with inversion of the configuration in the second step was obtained from a similar sequence of reactions of **4** with ClCH$_2$CO$_2$Me first, then with CN*t*Bu, and finally with R*Cl to give [(CN*t*Bu)$_2$(η^1-CH$_2$R)Rh(μ-NH{*p*-tolyl})$_2$(μ-Cl)Rh(η^1-R*)(CN*t*Bu)$_2$]Cl (R = CO$_2$Me, [**7**]Cl) as a single enantiomer with the *R* configuration at the chiral carbon. The reactions of **1** with (+)-(*S*)-XCH$_2$CH(CH$_3$)CH$_2$CH$_3$ (X = Br, I) gave the related complexes [{Rh(μ-NH{*p*-tolyl})(η^1-CH$_2$CH(CH$_3$)CH$_2$CH$_3$)(CN*t*Bu)$_2$}$_2$-(μ-X)]X, probably by following an S$_N$2 profile in both steps.

Keywords: amido-bridged complexes · chirality · chlorohydrocarbons · oxidative addition · rhodium

Introduction

The oxidative addition reaction of alkyl halides to low-valent transition-metal complexes is involved in several industrially important catalytic processes[1] and is a general synthetic method to form metal–carbon bonds.[2] Typically, the studies reported on these reactions deal with alkyl iodides and bromides.[3] In particular, the addition of methyl iodide to carbonyl rhodium and iridium complexes has been studied with mechanistic detail, since it is the key step in the Monsanto[4] process, and an intermediate step in the Cativa[4,5] process for the carbonylation of methanol. The oxidative addition reaction of alkyl chlorides to metal centers is far less common and more challenging than those of bromides and iodides. Moreover, these reactions involving volatile organochloro compounds, which are environmental pollutants, are of paramount interest: the search for their degradation[6] by either catalytic or stoichiometric reactions or biological systems has been stimulated. However, and in spite of this interest, complexes able to activate C–Cl bonds are uncommon. Until recently, some reported examples were phosphino complexes of palladium,[7] platinum,[8] and rhodium[9] in low oxidation states, cyclometalated complexes of platinum,[10] cyclopentadienyl derivatives of iridium,[11] and rhodium(I) compounds incorporating polydentate N-donor ligands,[12] sulfur macrocycles,[13] the disulfide anion,[14] $(S_2)^{2-}$, and basic phosphines such as PMe$_3$.[15] Recently, a

[a] Dr. C. Tejel, Prof. Dr. M. A. Ciriano, Dr. J. A. López, S. Jiménez, Dr. M. Bordonaba, Prof. L. A. Oro
Departamento de Química Inorgánica
Instituto de Ciencia de Materiales de Aragón
CSIC-Universidad de Zaragoza, Pedro Cerbuna 12
50009 Zaragoza (Spain)
Fax: (+34) 976-761-187
E-mail: ctejel@unizar.es

[b] Dr. J. A. López, Prof. L. A. Oro
Instituto Universitario de Catálisis Homogénea
Pedro Cerbuna 12, 50009-Zaragoza (Spain)

number of mechanistic studies on the addition of aryl chlorides to palladium phosphine complexes relevant to catalytic amination, disclosed by Buchwald and Hartwig, and cross-coupling reactions have been reported.[16]

Previous studies of our group on the topic have been based on dinuclear pyrazolate complexes of rhodium[17] and iridium[18] with isocyanides as ancillary ligands. The expanding use of transition-metal catalysts that employ nitrogen-donor ligands,[19] and the requirement of electron-rich rhodium centre for the oxidative addition of C–Cl bonds prompted us to test these reactions with the unusual amido-bridged dirhodium complexes recently reported.[20] In this paper we describe the results of their reactions with alkyl halides with special emphasis on the scrutiny of possible mechanisms for these reactions.

Results and Discussion

Treatment of the complex *syn*-[{Rh(μ-NH{*p*-tolyl})-(CN*t*Bu)$_2$}$_2$] (**1**) with ClCH$_2$CO$_2$Me produced addition of one molecule of the alkyl chloride to each metal centre to give the complex [{Rh(μ-NH{*p*-tolyl})(η^1-CH$_2$CO$_2$Me)-(CN*t*Bu)$_2$}$_2$(μ-Cl)]Cl ([**2**]Cl). The product of the reaction consists on a sole isomer with C_{2v} symmetry and a *syn–endo* configuration (Scheme 1), as deduced from the fairly simple

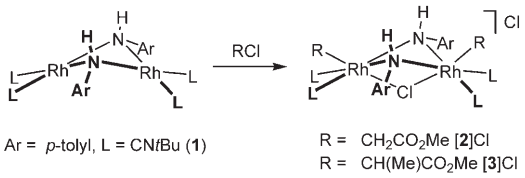

Scheme 1.

^{1}H and ^{13}C{^{1}H} NMR spectra. Thus, the attachment of two equivalent –CH$_2$CO$_2$Me groups to the rhodium atoms was evidenced by a doublet in the ^{1}H and ^{13}C{^{1}H} NMR spectra, due to the coupling of the methylenic protons and carbon with the ^{103}Rh active nucleus. In addition, the oxidation of both rhodium atoms to the Rh^{III}–Rh^{III} ([**2**]Cl) derivative was detected by a shift for the ν(CN) bands to higher frequencies (ca. 90 cm^{-1}) relative to **1** in the IR spectrum. Finally, the formulation of **2** as the chloro-bridged cation is supported by conductivity measurements of solutions of [**2**]Cl in acetone, which revealed it to be a 1:1 electrolyte.

Once we established the ability of complex **1** to react with activated alkyl chlorides, we explored the mechanistic features for this type of reaction by using chiral chlorocarbons, which could provide information about the Walden inversion expected in an S$_N$2 type reaction. A precedent for mechanistic studies of the addition of chiral alkylbromides to mononuclear iridium(I) complexes of the type [IrCl(CO)-(PR$_3$)$_2$] was previously reported by Osborn.[21] For this purpose, **1** was reacted with (–)-(*S*)-ClCH(Me)CO$_2$Me to give a white crystalline material analyzed as [{Rh(μ-NH{*p*-tolyl})-(η^1-CH(Me)CO$_2$Me)(CN*t*Bu)$_2$}$_2$(μ-Cl)]Cl ([**3**]Cl) (Scheme 1). The reaction was carried out in the dark, since it was found to be influenced by sunlight. When the reaction was carried out in light, [**3**]Cl also resulted, but it was contaminated with unknown compounds. Moreover, no radical trapping experiments could be carried out since the starting material reacts with radical scavengers, such as galvinoxyl, to give a dark purple insoluble material.

The crystalline material [**3**]Cl contained two cationic complexes in a 1:1 molar ratio, judging from the ^{1}H and ^{13}C{^{1}H} NMR spectra and conductivity measurements. One of the complexes, having C_s symmetry by NMR, was found to be the *meso* form (*R*,*S*)-[**3**]Cl-C_s, which was confirmed by a X-ray diffraction study. Figure 1 shows the structure of the cation (*R*,*S*)-[**3**]-C_s together with the atomic labeling scheme. Selected bond lengths and angles are collected in Table 1.

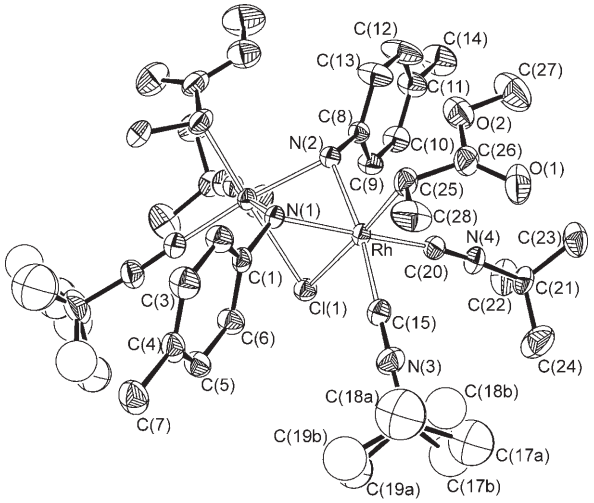

Figure 1. Molecular structure of the cation (*R*,*S*)-[**3**]-C_s.

Table 1. Selected bond lengths [Å] and angles [°] for the cation (*R*,*S*)-[{Rh(μ-NH{*p*-tolyl})(η^1-CH(Me)CO$_2$Me)(CN*t*Bu)$_2$}$_2$(μ-Cl)] {(*R*,*S*)-[**3**]-C_s}.

Rh···Rh′	2.9032(6)[a]	Rh–Cl(1)	2.5455(10)
Rh–N(1)	2.099(3)	Rh–N(2)	2.108(3)
Rh–C(15)	1.942(4)	Rh–C(20)	1.956(4)
Rh–C(25)	2.112(4)		
Cl(1)-Rh-N(1)	86.10(9)	Cl(1)-Rh-N(2)	85.57(9)
Cl(1)-Rh-C(15)	90.21(11)	Cl(1)-Rh-C(20)	89.04(10)
Cl(1)-Rh-C(25)	176.21(11)	Rh-Cl(1)-Rh′	69.54(3)
Rh-N(1)-Rh′	87.49(14)	Rh-N(2)-Rh′	87.06(14)

[a] Rh′ is related to Rh by the symmetry operation *x*, *y*, 1–*z*.

In the cation, two *p*-tolylamide ligands in a *syn–endo* configuration and a chloride group bridge two rhodium atoms. The coordination of each rhodium centre is essentially octahedral with an intermetallic separation of 2.9032(6) Å, similar to that found in complex **1**,[19b] but slightly shorter than those found in the complexes [{(η^5-Cp*)Rh(μ-NH{*p*-tolyl})}$_2$(μ-Cl)]$^+$ (3.101(1) Å)[22] and [{(η^5-Cp*)Rh(μ-naph)}$_2$-

(μ-Br)]$^+$ (3.04(2) Å).[23] The molecule possesses a crystallographic plane, which produces the equivalence of the two "Rh(η^1-CH(Me)CO_2Me)($CNtBu)_2$" moieties, confirming that the crystals contain the *meso* form (*R*,*S*)-[**3**]Cl-C_s.

The packing of the molecules in the crystal lattice is particularly interesting. It consists of infinite linear columns made of dinuclear entities, which in turn form four- and eight-membered alternated and superposed rings orthogonal to the columns, giving rise to empty inner channels, which represent a vacant space of about 11% in the structure. This leads to an abnormally low density of the crystals. A section of one of the channels perpendicular to the infinite columns is shown in Figure 2.

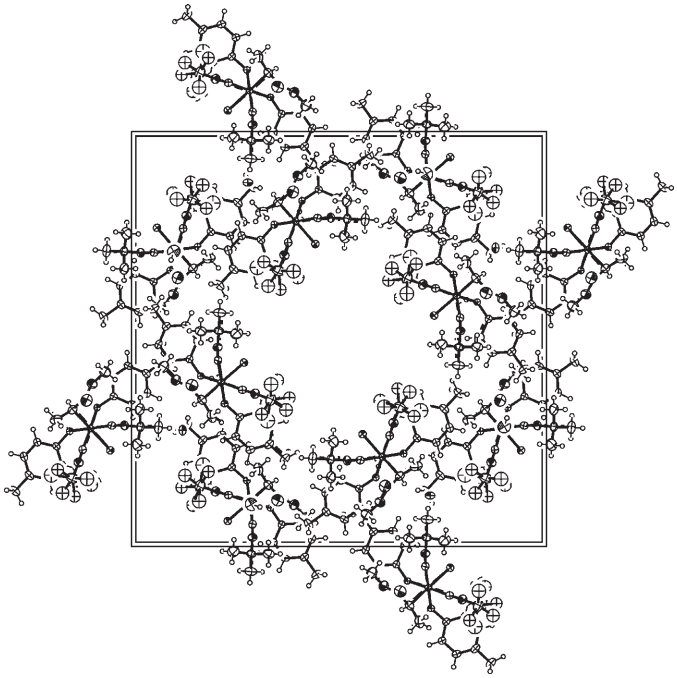

Figure 2. View of a section of the inner channel made up of the four- and eight-membered rings shown in the figure.

Furthermore, a water molecule of crystallization in the lattice binds two dinuclear entities through two hydrogen bonds to form the elementary linear infinite columns in the crystal packing. The hydrogen atoms of the water molecule almost linearly bridge the terminal oxygen atoms of the carboxylate groups [with separations of 2.06(7) and 3.009(5) Å for H···O and O···O, respectively].

The second product of the above reaction, having C_2 symmetry by NMR, could be the *R*,*R* isomer, the *S*,*S* isomer, or the racemic mixture. Measurements of the rotatory specific power of the crude product of the reaction gave a value of +23° indicating an enantiomeric excess of the *R*,*R* or *S*,*S* isomers of [**3**]Cl-C_2. Solutions of the crude product in hexadeuteroacetone (HAD) and $CDCl_3$ remained unaltered for 4 d, indicating that the diastereoisomers, (*R*,*S*)-[**3**]Cl-C_s and [**3**]Cl-C_2, did not interconvert and, consequently, the products obtained in a 1:1 molar ratio represented the result of the reaction of **1** with (−)-(*S*)-ClCH(Me)CO_2Me. Furthermore, addition of [Eu(hfc)$_3$] {hfc = 3-(heptafluoropropylhydroxymethylene)-(+)-camphorato} to a $CDCl_3$ solution of the crude product (C_s and C_2 isomers) did not split the resonances in the ^{1}H NMR spectrum, which suggested the [**3**]Cl-C_2 isomer was a single enantiomer. However, attempts to obtain monocrystals of [**3**]Cl-C_2 from the mother liquor were unsuccessful.

To ensure the ability of Eu(hfc)$_3$ to distinguish both enantiomers and, consequently, to establish that complex [**3**]Cl-C_2 was obtained as a sole enantiomer we proceeded as follows. Complex **1** was reacted with the racemic mixture (*R*+*S*)-ClCH(Me)CO_2Me to give a white material that corresponded to equimolar amounts of *R*,*S*-[**3**]Cl-C_s and (*R*,*R*+*S*,*S*)-[**3**]Cl-C_2. As expected, the rotatory specific power of the product was +0°. The ^{1}H NMR spectrum in $CDCl_3$ of this solid was clearly identical to that found in the reaction of **1** with (−)-(*S*)-ClCH(Me)CO_2Me. Addition of [Eu(hfc)$_3$] to this NMR tube produced the splitting of the resonances corresponding to the enantiomers (*R*,*R*)-[**3**]Cl-C_2 and (*S*,*S*)-[**3**]Cl-C_2. Therefore, the product of the reaction of **1** with (−)-(*S*)-ClCH(Me)CO_2Me was the complex (*R*,*S*)-[**3**]Cl-C_s and one enantiomer of the chiral-form [**3**]Cl-C_2 in equimolecular amounts. This result implies that the reaction takes place in two steps, one occurring with racemization of the chiral carbon, while the other is regioselective with either retention (to give (*S*,*S*)-[**3**]Cl-C_2) or inversion (to give (*R*,*R*)-[**3**]Cl-C_2) of the configuration of the chiral carbon in (−)-(*S*)-ClCH(Me)CO_2Me. Attempts to isolate the product from the oxidative addition of (−)-(*S*)-ClCH(Me)CO_2Me to one metal centre in **1** by using a 1:1 molar ratio were unsuccessful, resulting in a mixture of **1** and [**3**]Cl. This result, however, indicates that the second step of the reaction occurs faster than the first.

To disclose the features of the two steps, the overall reaction was modeled, step-by-step, following the strategy shown in Scheme 2. The first step was reproduced by using the mixed-ligand complex *syn*-[(cod)Rh(μ-NH{*p*-tolyl})$_2$Rh-($CNtBu)_2$] **4**, which is a model for complex **1** with the "Rh-(cod)" moiety protected from oxidative addition reactions.

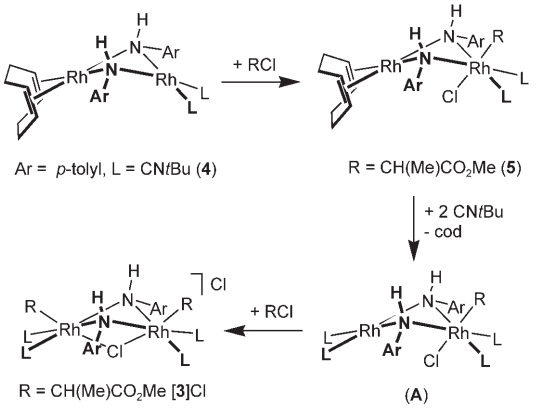

Scheme 2.

Complex **4** was easily accessible by reaction of [{Rh(μ-NH{*p*-tolyl})(cod)}$_2$] with two molar equivalents of CN*t*Bu in diethyl ether. Analytical and spectroscopic data (see Experimental Section) agreed with the proposed formulation for **4**. Treatment of a toluene suspension of **4** with (−)-(*S*)-ClCH(Me)CO$_2$Me gave the neutral complex [(cod)Rh(μ-NH{*p*-tolyl})$_2$RhCl(η^1-CH(Me)CO$_2$Me)(CN*t*Bu)$_2$] (**5**) (Scheme 2), which was isolated as yellow monocrystals. As anticipated, the addition of (−)-(*S*)-ClCH(Me)CO$_2$Me to **4** was found to occur at only one metal centre, the rhodium atom with isocyanide ligands, as shown by the shift of ν(CN) at about 90 cm^{-1} to higher frequencies relative to **4**.

Complex **5** showed broad signals in the ^{1}H NMR spectrum at room temperature, as due to a fluxional species, but the motion was slowed down at −50 °C. At this temperature the bridging ligands were found to be inequivalent, giving four AB spin systems for the aromatic *p*-tolylamide protons in the ^{1}H NMR spectrum, which indicated freezing of the rotation of the phenyl rings about the C–N bonds. Accordingly, the ^{13}C{^{1}H} NMR spectrum showed twelve resonances for the aromatic carbons, as expected for a species lacking elements of symmetry, while the -CH(Me)CO$_2$Me group gave four signals, the doublet corresponding to the carbon directly bonded to rhodium (see Experimental Section). Measurements of the rotatory specific power of these crystals showed a value close to zero, indicating that **5** was a racemic mixture, which was confirmed by an X-ray diffraction study. Figure 3 shows the structure of one of the two enantiomers found in the crystals of **5** together with the atomic labeling scheme. Selected bond lengths and angles are collected in Table 2.

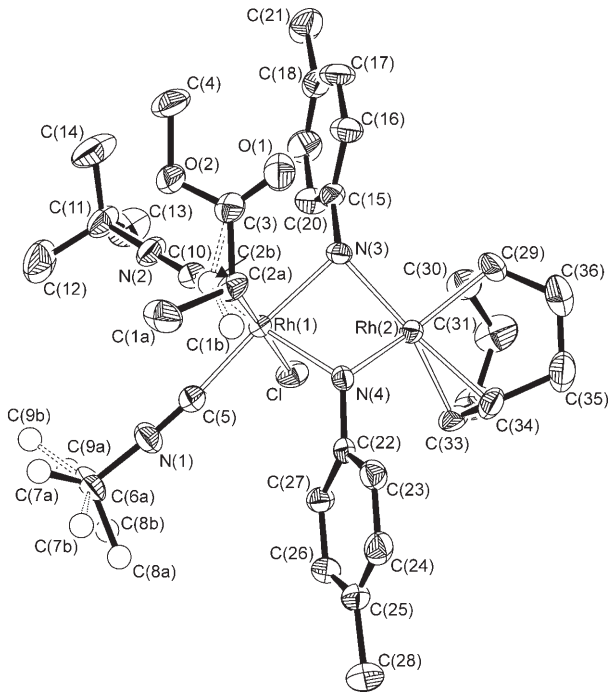

Figure 3. Molecular structure of complex **5**.

Table 2. Selected bond lengths [Å] and angles [°] for (*R*+*S*)-[(cod)Rh(μ-NH{*p*-tolyl})$_2$RhCl(η^1-CH(Me)CO$_2$Me)(CN*t*Bu)$_2$] (**5**).

Rh(1)···Rh(2)	3.0327(5)	Rh(1)–Cl	2.5258(9)
Rh(1)–N(3)	2.116(3)	Rh(1)–N(4)	2.093(3)
Rh(1)–C(5)	1.951(4)	Rh(1)–C(10)	1.944(4)
Rh(1)–C(2a)	2.152(9)	Rh(1)–C(2b)	2.10(3)
Rh(2)···Cl	3.0493(11)	Rh(2)–N(3)	2.134(3)
Rh(2)–N(4)	2.168(3)	Rh(2)–C(29)	2.081(4)
Rh(2)–C(30)	2.111(4)	Rh(2)–C(33)	2.103(3)
Rh(2)–C(34)	2.125(3)		
Cl-Rh(1)-N(3)	90.92(8)	Cl-Rh(1)-N(4)	90.15(7)
Cl-Rh(1)-C(5)	87.03(11)	Cl-Rh(1)-C(10)	87.14(11)
Cl-Rh(1)-C(2a)	176.94(18)	Cl-Rh(1)-C(2b)	168.0(5)
N(3)-Rh(2)-N(4)	75.99(10)	M(1)-Rh(2)-M(2)[a]	88.32(19)
N(3)-Rh(2)-M(1)	97.86(16)	N(4)-Rh(2)-M(1)	164.67(13)
N(3)-Rh(2)-M(2)	173.74(16)	N(4)-Rh(2)-M(2)	97.76(14)
Rh(1)-N(3)-Rh(2)	91.06(10)	Rh(1)-N(4)-Rh(2)	90.74(10)

[a] M(1) and M(2) are the mid-points between C(29)–C(30) and C(33)–C(34), respectively.

In the complex, the rhodium atoms are bridged by two amido ligands in a *syn–endo* configuration. The rhodium atom in the "Rh^{I}(cod)" moiety shows square-planar coordination, while the rhodium(III) centre is in a pseudo-octahedral environment with the CH(Me)CO$_2$Me group *trans* to the chloride ligand, which is inside the pocket of the molecule. The chiral fragment is disordered into two conformations of opposite chirality [C(1a) and C(2a), 0.732(12) occupancy factor; C(1b) and C(2b), 0.268(12) occupancy factor], but because the space group is centrosymmetric (*P*1), the crystal contains a racemic mixture. The folding of the structure, defined by the dihedral angle of 131.2(1)° between the N(3)-Rh(1)-N(4) and N(3)-Rh(2)-N(4) planes is very similar to that reported for the related Rh^{I} complexes [{Rh(μ-NH{*p*-tolyl})(cod)}$_2$] and [{Rh(μ-NH{*p*-tolyl})(CN*t*Bu)$_2$}$_2$], with values of 131.9(2) and 134.16(12)°, respectively.[19b]

In consequence, the reaction of *syn*-[(cod)Rh(μ-NH{*p*-tolyl})$_2$Rh(CN*t*Bu)$_2$] **4** with (−)-(*S*)-ClCH(Me)CO$_2$Me occurs with racemization of the chiral carbon of the chloro-derivative.

Continuing with the strategy shown in Scheme 2, complex **5** was treated with two molar equivalents of CN*t*Bu to give the intermediate [(CN*t*Bu)$_2$Rh(μ-NH{*p*-tolyl})$_2$RhCl(η^1-CH(Me)CO$_2$Me)(CN*t*Bu)$_2$] (**A**, Scheme 2). Since the replacement of cod by CN*t*Bu deprotects the Rh^{I} centre in **5** for oxidative addition reactions, **A** was reacted in situ with (−)-(*S*)-ClCH(Me)CO$_2$Me. The result of this reaction was identical {(*R*,*S*)-[**3**]Cl-C_s and [**3**]Cl-C_2 in 1:1 molar ratio} to that obtained from the direct reaction of **1** with (−)-(*S*)-ClCH(Me)CO$_2$Me. Thus, the sequence of reactions shown in Scheme 2 replicates stepwise the direct reaction shown in Scheme 1. Consequently, it can be concluded that the first step in the reaction of **1** with (−)-(*S*)-ClCH(Me)CO$_2$Me takes place with racemization of the chiral carbon and that the second step is the regioselective one.

To determine which enantiomer results from the second step, the active rhodium atom in the mixed-ligand complex **4** was first oxidized with ClCH$_2$CO$_2$Me, a nonchiral compound, to give the mixed-valence Rh^{I}–Rh^{III} complex

[(cod)Rh(μ-NH{*p*-tolyl})$_2$RhCl(η^1-CH_2CO_2Me)(CN*t*Bu)$_2$] (**6**). Complex **6** was found to be a fluxional species like **5**, but the frozen structure was identified as the species having a *syn–endo* configuration and a plane of symmetry by NMR spectroscopy at −90 °C. Then, the unreactive rhodium atom in **6** (from the "Rh(cod)" moiety) was activated by adding two molar equivalents of CN*t*Bu, which was finally reacted with (−)-(*S*)-ClCH(Me)CO_2Me. The resulting white crystalline material was found to be the complex [(CN*t*Bu)$_2$(η^1-CH_2R)Rh(μ-NH{*p*-tolyl})$_2$(μ-Cl)Rh(η^1-CH(Me)R)(CN*t*Bu)$_2$]-Cl (R = CO_2Me, [**7**]Cl). Complex [**7**]Cl was identified by ^{1}H and ^{13}C{^{1}H} NMR spectroscopy as the sole compound lacking symmetry elements, with the -$CHCO_2$Me and -CH(Me)CO_2Me fragments each bonded to one rhodium atom. Moreover, the most relevant feature of the reaction was that [**7**]Cl was obtained as a single enantiomer. This was clearly revealed by the lack of splitting of the signals in the ^{1}H NMR spectrum upon addition of [Eu(hfc)$_3$], and the measured value of the rotatory specific power of [**7**]Cl (+22°). Attempts to obtain monocrystals of [**7**]Cl gave, systematically, merohedric twins of difficult resolution. However, monocrystals of the triflate salt [**7**]Tf suitable for X-ray diffraction studies were obtained by reacting [**7**]Cl with one molar equivalent of methyltriflate (MeTf), which released the chloride anion as MeCl. Figure 4 shows the molecular structure of the cation **7** together with the atomic labeling scheme. Selected bond lengths and angles are collected in Table 3.

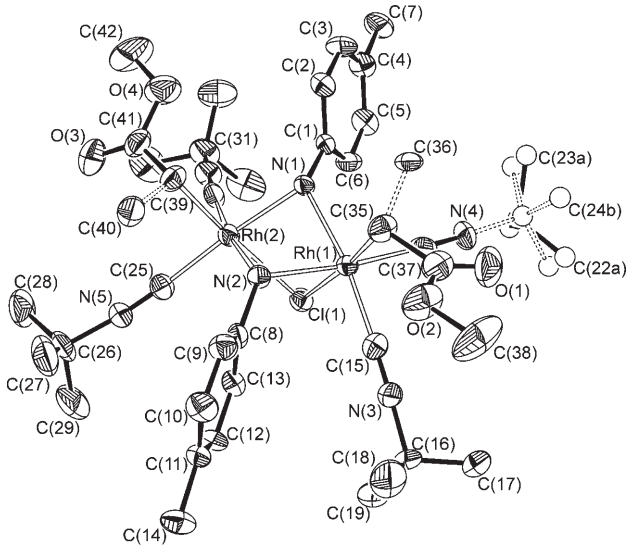

Figure 4. Molecular structure of the cation **7**.

The structure of **7** was found to be the expected dinuclear complex with -$CHCO_2$Me and -CH(Me)CO_2Me fragments, the latter having an *R* configuration at the chiral carbon as the most relevant feature. The alkyl fragments were found to be disordered in such a way that the chiral one, -CH(Me)CO_2Me, is bonded to Rh(2) (with a 0.59(16) occupancy factor) and to Rh(1) (with a 0.41(16) occupancy factor), but with identical absolute configuration of the chiral carbon atom (C(35) and C(39)).

Table 3. Selected bond lengths [Å] and angles [°] for [(CN*t*Bu)$_2$(η^1-CH_2CO_2Me)Rh(μ-NH{*p*-tolyl})$_2$(μ-Cl)Rh(η^1-CH(Me)CO_2Me)(CN*t*Bu)$_2$]-OTf ([**7**]OTf).

Rh(1)···Rh(2)	2.9233(8)	Rh(2)−Cl(1)	2.5443(17)
Rh(1)−Cl(1)	2.5218(17)	Rh(2)−N(1)	2.109(5)
Rh(1)−N(1)	2.101(5)	Rh(2)−N(2)	2.090(5)
Rh(1)−N(2)	2.121(5)	Rh(2)−C(25)	1.949(7)
Rh(1)−C(15)	1.942(7)	Rh(2)−C(30)	1.958(8)
Rh(1)−C(20)	1.969(8)	Rh(2)−C(39)	2.108(7)
Rh(1)−C(35)	2.096(7)		
Cl(1)-Rh(1)-N(1)	84.27(14)	Cl(1)-Rh(2)-N(1)	83.56(14)
Cl(1)-Rh(1)-N(2)	84.69(15)	Cl(1)-Rh(2)-N(2)	84.76(15)
Cl(1)-Rh(1)-C(15)	92.8(2)	Cl(1)-Rh(2)-C(25)	96.0(2)
Cl(1)-Rh(1)-C(20)	94.2(2)	Cl(1)-Rh(2)-C(30)	90.7(2)
Cl(1)-Rh(1)-C(35)	174.8(2)	Cl(1)-Rh(2)-C(39)	172.84(19)
Rh(1)-N(1)-Rh(2)	87.96(18)	Rh(1)-N(2)-Rh(2)	87.92(19)
Rh(1)-Cl(1)-Rh(2)	70–48(4)		

The addition of (−)-(*S*)-ClCH(Me)CO_2Me to the mixed-valence intermediate [(CN*t*Bu)$_2$Rh(μ-NH{*p*-tolyl})$_2$RhCl(η^1-CH_2CO_2Me)(CN*t*Bu)$_2$] therefore takes place with an inversion of the configuration at the chiral carbon. This result strongly supports an S_N2 type reaction for the second step, which is associated with a Walden inversion at the chiral carbon. Most probably, the isolated enantiomer [**3**]Cl-C_2 is then (*R*,*R*)-[**3**]Cl-C_2.

These results are incorporated in the proposed mechanism shown in Scheme 3 for the oxidative addition of (−)-(*S*)-ClCH(Me)CO_2Me to **1**, which accounts for the observed features. The racemic compound (*R*+*S*)-[(CN*t*Bu)$_2$Rh(μ-NH{*p*-tolyl}$_2$RhCl(η^1-CH(Me)CO_2Me)(CN*t*Bu)$_2$] **A** is produced in the first step, most probably through a radical mechanism. We believe that the initial step consists of halide abstraction from the chlorocarbon to give the radical pair [{Rh(μ-NH{*p*-tolyl})(CN*t*Bu)$_2$}$_2$Cl]$^{\bullet}$[CH(Me)CO_2Me]$^{\bullet}$,

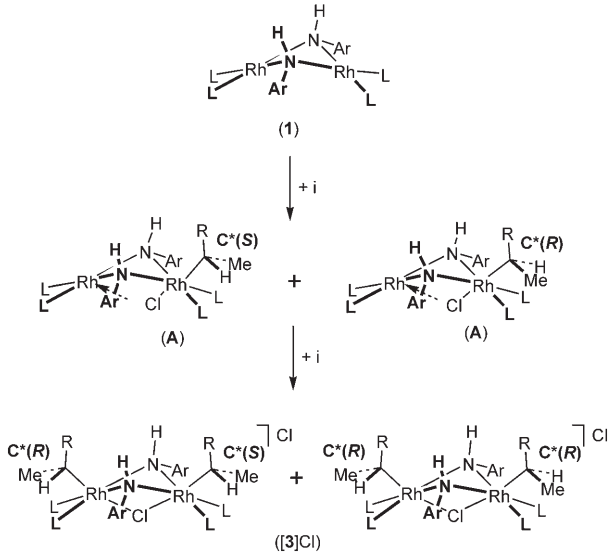

Scheme 3. i) = (−)-(*S*)-ClCH(Me)CO_2Me, R = CO_2Me.

since this allows the epimerization of the chiral carbon before the radical pair collapses into the intermediate **A**. An alternative S_N1 type reaction seems to be rather improbable, since all reactions were carried out in nonpolar solvents such as diethyl ether or toluene. The second step takes place through an S_N2 type reaction, which leads to the two diastereoisomers (*R*,*R*)-[**3**]Cl-C_2 and (*R*,*S*)-[**3**]Cl-C_s in a 1:1 molar ratio, as experimentally observed.

The complexes **1** and **4** are reactive enough to add one molar equivalent of dichloromethane, immediately upon mixing with this chemical used as solvent, to give the methylene-bridged complexes *anti*-[{RhCl(μ-NH{*p*-tolyl})-(CN*t*Bu)$_2$}$_2$(μ-CH$_2$)] (**8**, Scheme 4), and *syn*-[(cod)ClRh(μ-CH$_2$)(μ-NH{*p*-tolyl})$_2$RhCl(CN*t*Bu)$_2$] (**9**, Scheme 4), in good

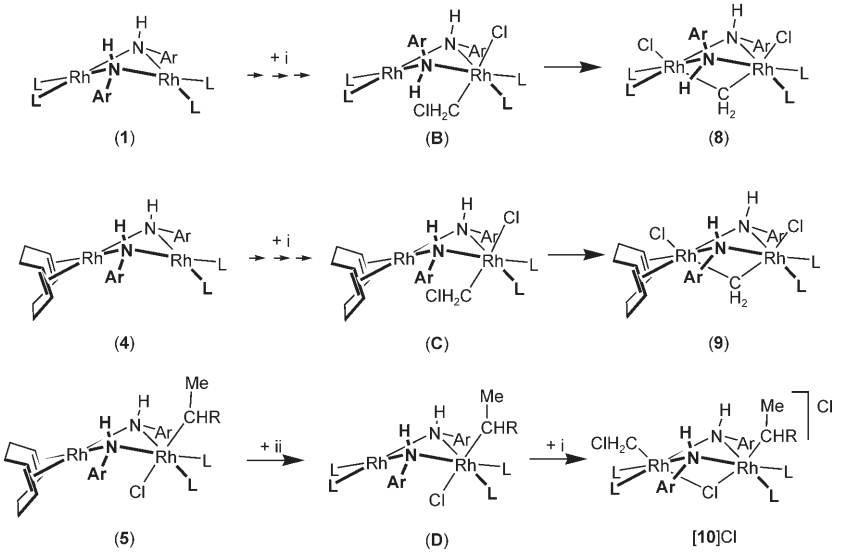

Scheme 4. Ar = *p*-tolyl, L = CN*t*Bu, R = CO$_2$Me, i) CH$_2$Cl$_2$, ii) 2 CN*t*Bu.

yields. Conclusive evidence for the methylene groups bridging the rhodium atoms is a triplet in the $^{13}C\{^1H\}$ NMR spectra that is due to the coupling of the carbon to two rhodium nuclei. The most significant difference between **8** and **9** is the *syn* or *anti* disposition of the *p*-tolyl groups, which are *anti* in **8** and *syn* in **9**, as deduced from the NMR spectra.

The methylene group results from a three-fragment four-electron oxidative addition of dichloromethane to complexes **1** and **4**. Most probably, these reactions take place in two steps, and it is reasonable to propose that the first step renders the mixed-valence complexes Rh^{I}–Rh^{III} with the chloromethyl ligand bonded to the rhodium centre with the coordinated isocyanide ligands (Scheme 4). The second step involves an internal oxidative addition of the chloromethyl ligand to the neighboring Rh^{I} centre in such a way that the reaction is accomplished with the formation of the methylene bridge (Scheme 4).

Noticeably, this second step is rather faster than a possible oxidative addition of a second molecule of dichloromethane to the Rh^{I} centre in the mixed-valence intermediate, even if this chemical is the solvent. To check this possibility, the mixed-valence complex [(cod)Rh(μ-NH{*p*-tolyl})$_2$RhCl(η^1-CH(Me)CO$_2$Me)(CN*t*Bu)$_2$] (**5**) was reacted with CN*t*Bu in dichloromethane as solvent to cleanly give the chloromethyl-complex [(CN*t*Bu)$_2$(η^1-CH$_2$Cl)Rh(μ-NH{*p*-tolyl})$_2$(μ-Cl)Rh(η^1-CH(Me)CO$_2$Me)(CN*t*Bu)$_2$]Cl ([**10**]Cl) (see Experimental Section), resulting from the addition of dichloromethane to a single rhodium centre. Thus, although dichloromethane does not add to **5**, it does add to the mixed-valence Rh^{I}–Rh^{III} complex generated "in situ", [(CN*t*Bu)$_2$Rh(μ-NH{*p*-tolyl})$_2$RhCl(η^1-CH(Me)CO$_2$Me)(CN*t*Bu)$_2$] (**D**), to produce the chloromethyl ligand.

Moreover, the product [**10**]Cl possesses a structure similar to that of the complexes [**2**]Cl, [**3**]Cl, and [**7**]Cl, which result from the double addition of a monocloroalkane to **1** in two separate steps, as commented above. This experiment also demonstrates that intermediates of the type **D** are able to add dichloromethane. Therefore, one could expect that reactions of **1** with dichloromethane give the product of the double oxidative addition with two chloromethyl groups, such as [{(CN*t*Bu)$_2$(η^1-CH$_2$Cl)Rh(μ-NH{*p*-tolyl})$_2$}$_2$(μ-Cl)]Cl. However, this compound was not observed in the crude product from the reaction of **1** with dichloromethane. This observation strongly supports the participation of the intermediates **B** and **C** (Scheme 4) in these reactions. Species **B** and **C** contain the chloromethyl ligand inside the pocket of the complex and close to the unreacted Rh^{I} centre, which allows a fast internal addition reaction with the Rh^{I} centre to give the methylene-bridged complexes **8** and **9**, satisfying the three-fragment four-electron scheme. Since complexes **8** and **9** do not isomerize into the *syn* or *anti* configurations, respectively, we believe that the configurations of the mixed-valence Rh^{I}–Rh^{III} intermediates **B** and **C** are those shown in Scheme 4. Probably, intermediates of this type might also be formed in the reactions of **1** and **4** with monochloro derivatives. In such a case, they isomerize to the thermodynamic products containing the alkyl group outside the pocket of the complex, as observed for complexes **5** and **6**.

Another remarkable feature of these reactions can be found by analyzing the formation of complex **9**. The "Rh(cod)" moiety in **5** is unable to cleave the C–Cl bond of an external dichloromethane molecule; whereas in the intermediate **C**, this moiety reacts with a chloromethyl fragment coordinated to the neighboring rhodium atom and placed inside of the pocket of the complex, providing an example of a "bimetallic activation" process.

Finally, to gain further information about the reactions of complex **1** with bromo- and iodo derivatives and about pos-

sible mechanistic pathways, the reactions of **1** with the commercially available primary alkyl halides possessing a chiral carbon at the β-position (+)-(*S*)-X-CH_2-$CH(CH_3)CH_2CH_3$ (X = Br, I) were also studied. These reactions proceeded smoothly to give the complexes [{Rh(μ-NH{*p*-tolyl})(η^1-$CH_2CH(CH_3)CH_2CH_3$)($CNtBu)_2$}$_2$(μ-X)]X (X = Br, [**11**]Br; X = I, [**12**]I) coming from the oxidative addition reaction of two molar equivalents of the alkyl halide. Both products were obtained as a single enantiomer with C_2 symmetry, according to the analytical and spectroscopic data. Additionally, an X-ray diffraction study of complex [**12**]I confirmed the chirality at the β-carbon remained unaltered in these reactions. Figure 5 shows the molecular structure of the cation **12** together with the atomic labeling scheme used for one of the almost identical two independent molecules. Selected bond lengths and angles are collected in Table 4. Complex [**12**]I crystallizes in the noncentrosymmetric *P*1 space group,

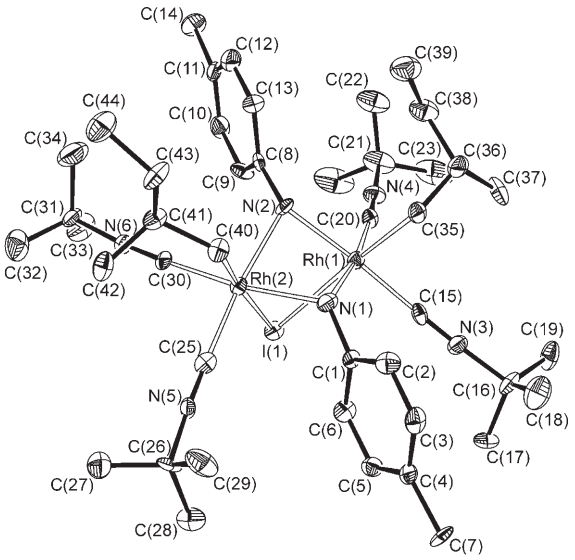

Figure 5. Molecular structure of the cation **12**.

although there is a pseudocentre of symmetry that relates the two molecules, except the chiral groups, in which the β-carbon has the *S* configuration.

The maintenance of the chirality at the β-carbon in products [**11**]Br and [**12**]I is a clear indication of an S_N2 profile in the two oxidative addition steps that afford the products. Indeed, if radical pairs of the type [{Rh(μ-NH{*p*-tolyl})-($CNtBu)_2$}$_2$X]$^{\bullet}$[CH_2-$CH(CH_3)CH_2CH_3$]$^{\bullet}$ were intermediates, a fast 1,2-prototropic shift producing the tertiary radical [CH_3–$C(CH_3)CH_2CH_3$)]$^{\bullet}$ should be expected. Under these conditions, the products should have either the Rh–$C(Me)_2CH_2CH_3$ moiety or the Rh–CH_2–$CH(CH_3)CH_2CH_3$ fragment with the β-carbon epimerized to some extent. Identical products would be expected if the reactions were to follow an S_N1 type mechanism profile involving the corresponding carbocations. Consequently, the reactions of **1** with the alkyl halides (+)-(*S*)-XCH_2-$CH(CH_3)CH_2CH_3$ (X = Br, I) probably follow an S_N2 mechanism in both steps.

Table 4. Selected bond lengths[a] [Å] and angles [°] for the cation **12**.

Rh(1)···Rh(2)	2.9199(9) [2.9198(9)]		
Rh(1)–I(1)	2.9091(7) [2.8995(8)]	Rh(2)–I(1)	2.8966(8) [2.9095(7)]
Rh(1)–N(1)	2.101(7) [2.111(6)]	Rh(2)–N(1)	2.104(7) [2.122(6)]
Rh(1)–N(2)	2.103(6) [2.094(6)]	Rh(2)–N(2)	2.110(6) [2.091(7)]
Rh(1)–C(15)	1.936(8) [1.932(8)]	Rh(2)–C(25)	1.949(8) [1.952(8)]
Rh(1)–C(20)	1.939(8) [1.911(8)]	Rh(2)–C(30)	1.969(8) [1.946(8)]
Rh(1)–C(35)	2.127(7) [2.089(7)]	Rh(2)–C(40)	2.081(7) [2.075(7)]
Rh(1)-I(1)-Rh(2)	60.39(2) [60.35(2)]	Rh(1)-N(1)-Rh(2)	88.0(2) [87.2(2)]
Rh(1)-N(2)-Rh(2)	87.8(2) [88.5(2)]	I(1)-Rh(1)-N(1)	88.26(18) [89.81(17)]
I(1)-Rh(2)-N(1)	88.53(18) [89.33(17)]	I(1)-Rh(1)-N(2)	88.02(18) [88.02(18)]
I(1)-Rh(2)-N(2)	88.22(17) [87.82(17)]	I(1)-Rh(1)-C(15)	93.0(2) [93.8(2)]
I(1)-Rh(2)-C(25)	95.0(2) [93.0(2)]	I(1)-Rh(1)-C(20)	89.1(2) [89.2(2)]
I(1)-Rh(2)-C(30)	89.7(2) [89.4(2)]	I(1)-Rh(1)-C(35)	173.3(2) [171.9(2)]
I(1)-Rh(2)-C(40)	175.4(2) [176.5(2)]		

[a] The two values for each entry correspond to the two independent molecules.

Conclusion

In summary, we have proved that the double oxidative addition reactions of some chloroalkanes to dinuclear amidorhodium complexes occur in two steps. The first step follows a one-electron mechanism involving free radicals, while the second occurs with a Walden inversion at the chiral carbon, according to a two-electron mechanism (of the S_N2 or S_Ni type). However, the corresponding reactions with related bromo-and iodoalkanes follow an S_N2 mechanism in both steps.

Experimental Section

General: All reactions were carried out under argon using standard Schlenk techniques. The complex [{Rh(μ-NH{*p*-tolyl})($CNtBu)_2$}$_2$] was prepared according to literature methods.[20b] Solvents were dried and distilled under argon by standard methods before use. Carbon, hydrogen, and nitrogen analyses were performed using a Perkin–Elmer 2400 microanalyzer. IR spectra were recorded with a Nicolet 550 spectrophotometer. Mass spectra were recorded with a VG Autospec double-focusing mass spectrometer operating in the FAB+ mode. Ions were produced with the standard Cs+ gun at about 30 KV, 3-nitrobenzyl alcohol (NBA) was used as matrix. ^{1}H and ^{13}C{^{1}H} NMR spectra were recorded on a Bruker ARX 300 and a Varian UNITY 300 spectrometers operating at 300.13 and 299.95 MHz, respectively, for ^{1}H. Chemical shifts are reported

in parts per million and referenced to $SiMe_4$ using the signal of the deuterated solvent as reference.

[{Rh(μ-NH{*p*-tolyl})(η¹-CH_2CO_2Me)(CN*t*Bu)$_2$}$_2$(μ-Cl)]Cl ([2]Cl): Methylchloroacetate (25.2 μL, 0.28 mmol) was added to a suspension of **1** (100.0 mg, 0.13 mmol) in diethyl ether (15 mL) at room temperature. After stirring for 2 h, the resulting suspension was left in the refrigerator for 2 d to render a white microcrystalline solid, which was filtered off, washed with diethyl ether (2×5 mL), and vacuum-dried (105.3 mg, 83 %). ^{1}H NMR ($CDCl_3$, 25 °C): δ = 7.50 (δA, 4H) and 6.97 (δB, J(A,B) = 8.2 Hz, 4H; *p*-MeC_6H_4), 3.52 (s, 6H; CO_2Me), 2.85 (s, 2H; NH), 2.35 (d, ^2J(H,Rh) = 3.4 Hz, 4H; Rh−CH_2), 2.22 (s, 6H; *p*-$Me$$C_6H_4$), 1.21 ppm (s, 36H; *t*Bu); ^{13}C{^{1}H} NMR ($CDCl_3$, 25 °C): δ = 178.6 (s; CO_2Me), 153.7 (Ci), 132.9 (C*p*), 129.0 (C*m*), 121.7 (C*o*), 58.7 ($C(CH_3)_3$), 51.4 (CO_2Me), 29.7 (C(CH_3)$_3$), 20.6 (*p*-$Me$$C_6H_4$), 11.3 ppm (d, J(C,Rh) = 25 Hz, Rh−CH_2); IR (CH_2Cl_2): ν = 2220 (s), 2201 cm^{-1} (s; CN); MS: *m*/*z* (%): 931 (100) [M^+]; Λ_M (3×10^{-4} M in acetone) = 108.3 S mol^{-1} cm^{-1}; elemental analysis calcd (%) for $C_{40}H_{62}N_6Cl_2O_4Rh_2$ (967.7): C 49.65, H 6.46, N 8.68; found: C 49.48, H 6.51, N 8.71.

[{Rh(μ-NH{*p*-tolyl})(η¹-CH(Me)CO_2Me)(CN*t*Bu)$_2$}$_2$(μ-Cl)]Cl ([3]Cl): (−)-(*S*)-2-Methylchloropropionate (200.0 μL, 1.42 mmol) was added in the dark to a suspension of **1** (100.0 mg, 0.13 mmol) in diethyl ether (10 mL). After stirring for 24 h, the white suspension was left in the refrigerator for 2 d. The white microcrystalline solid deposited was filtered off, washed with diethyl ether (2×5 mL), and vacuum-dried (112.7 mg, 85 %). Single crystals of [**3**]Cl-C_s were grown from a concentrated solution of [**3**]Cl in dichloromethane layered with diethyl ether. ^{1}H NMR ($CDCl_3$, 25 °C): isomer (*R*,*R*)-[**3**]Cl-C_2: δ = 7.50 (m, 4H) and 6.96 (m, 4H; *p*-MeC_6H_4), 3.51 (s, 6H; CO_2Me), 3.07 (m, 2H; Rh−C*H*Me), 2.79 (s, 2H; NH), 2.24 (s, 6H; *p*-$Me$$C_6H_4$), 1.28 (s, 18H) and 1.24 (s, 18H; *t*Bu), 1.06 ppm (dd, 6H, ^3J(H,H) = 6.6, ^3J(H,Rh) = 2.4 Hz; Rh−CHMe); isomer (*R*,*S*)-[**3**]Cl-C_s: δ = 7.50 (m, 4H) and 6.96 (m, 4H; *p*-MeC_6H_4), 3.53 (s, 6H; CO_2Me), 3.07 (m, 2H; Rh−C*H*Me), 3.03 (s, 1H) and 2.59 (s, 1H; NH), 2.25 (s, 3H) and 2.23 (s, 3H; *p*-$Me$$C_6H_4$), 1.28 (s, 18H) and 1.24 (s, 18H; *t*Bu), 1.05 ppm (dd, 6H, ^3J(H,H) = 6.6, ^3J(H,Rh) = 2.4 Hz; Rh−CHMe); ^{13}C{^{1}H} NMR ($CDCl_3$, 25 °C): isomer (*R*,*R*)-[**3**]Cl-C_2: δ = 179.7 (d, ^2J(C,Rh) = 2 Hz; CO_2Me), 153.9 (Ci), 132.7 (C*p*), 128.7 (C*m*), 122.3 (C*o*), 58.6 ($C(CH_3)_3$), 51.4 (CO_2Me), 29.7 and 29.6 (C(CH_3)$_3$), 24.4 (d, J(C,Rh) = 25 Hz; Rh−C*H*Me), 21.8 (d, ^2J(C,Rh) = 1 Hz; Rh−CHMe), 21.6 ppm (*p*-$Me$$C_6H_4$); isomer (*R*,*S*)-[**3**]Cl-C_s: δ = 179.8 (d, ^2J(C,Rh) = 2 Hz; CO_2Me), 154.0 and 153.6 (Ci), 132.8 and 132.6 (C*p*), 129.0 and 128.4 (C*m*), 122.6 and 122.1 (C*o*), 58.5 ($C(CH_3)_3$), 52.1 (CO_2Me), 29.5 (C(CH_3)$_3$), 24.2 (d, J(C,Rh) = 25 Hz; Rh−C*H*Me), 21.7 (d, ^2J(C,Rh) = 1 Hz; Rh−CHMe), 20.63 and 20.58 ppm (*p*-$Me$$C_6H_4$); IR ($CH_2Cl_2$): ν = 2220 (s), 2199 cm^{-1} (s; CN); MS: *m*/*z* (%): 959 (100) [M^+]; Λ_M (5 10^{-4} M in acetone) = 107.9 S mol^{-1} cm^{-1}; elemental analysis calcd (%) for $C_{42}H_{66}N_6Cl_2O_4Rh_2$ (995.7): C 50.66, H 6.68, N 8.44; found: C 50.33, H 6.54, N 8.44.

[(cod)Rh(μ-NH{*p*-tolyl})$_2$Rh(CN*t*Bu)$_2$] (4): CN*t*Bu (105.0 μL, 0.95 mmol) was slowly added to a suspension of [{Rh(μ-NH{*p*-tolyl})(cod)}$_2$] (300.0 mg, 0.47 mmol) in diethyl ether (15 mL). After stirring for 4 h, the resulting suspension was concentrated to about 5 mL and hexane (10 mL) was added to complete the crystallization. The yellow microcrystalline solid was filtered under argon, washed with hexane (2×5 mL), and dried under vacuum (240.4 mg, 74 %). ^{1}H NMR ([D$_6$]benzene, 25 °C): δ = 7.13 (δA, 4H) and 6.91 (δB, J(A,B) = 7.8 Hz, 4H; *p*-MeC_6H_4), 3.81 (m, 2H) and 3.52 (m, 2H; =CH cod), 2.43 (m, 2H) and 2.21 (m, 2H; CH_2*exo* cod), 2.20 (s, 6H; *p*-$Me$$C_6H_4$), 1.97 (s, 2H; NH), 1.59 (m, 4H; CH_2*endo* cod), 0.92 ppm (s, 18H; *t*Bu); ^{13}C{^{1}H} NMR ([D$_6$]benzene, 25 °C): δ = 155.7, 127.6, 127.1 and 122.0 (*p*-MeC_6H_4), 78.1 (d, J(C,Rh) = 13 Hz) and 77.1 (d, J(C,Rh) = 13 Hz; =CH cod), 54.9 (C(CH_3)$_3$), 31.3 and 30.3 (CH_2 cod), 30.2 (C(CH_3)$_3$), 20.5 ppm (*p*-$Me$$C_6H_4$); IR (cyclohexane): ν = 2131 (s), 2100 (w), 2064 (m), 2056 cm^{-1} (s; CN); MS: *m*/*z* (%): 692 (25) [M^+]; elemental analysis calcd (%) for $C_{32}H_{46}N_4Rh_2$ (692.6): C 55.50, H 6.69, N 8.09; found: C 55.28, H 6.54, N 8.44.

[(cod)Rh(μ-NH{*p*-tolyl})$_2$RhCl(η¹-CH(Me)CO_2Me)(CN*t*Bu)$_2$] (5): (−)-(*S*)-2-Methylchloropropionate (120.0 μL, 0.86 mmol) was added in the dark to a suspension of **4** (100.0 mg, 0.14 mmol) in toluene (8 mL). After stirring for 24 h the resulting yellow solution was concentrated to about 2 mL and carefully layered with hexane (15 mL). The yellow crystals deposited after two days, suitable for X-ray diffraction studies, were filtered off washed with hexane (2×5 mL) and vacuum dried (90.3 mg, 77 %). ^{1}H NMR (CD_2Cl_2, −50 °C) (assigned from the ^{1}H,^{1}H-COSY spectrum): δ = 8.04 (dd, J(H,H) = 8.4, 2.1 Hz, 1H; H*1a*), 7.98 (dd, J(H,H) = 8.1, 1.8 Hz, 1H; H*1b*), 6.95 (m, 2H; H*2a*+*2b*), 6.72 (m, 2H; H*3a*+*3b*), 6.61 (dd, J(H,H) = 8.4, 2.1 Hz, 1H; H*4b*) and 6.58 (dd, J(H,H) = 8.4, 2.1 Hz, 1H; H*4a*; *p*-MeC_6H_4), 3.31 (s, 3H; CO_2Me), 3.05 (brs, 3H) and 2.98 (brs, 1H; =CH cod), 2.67 (m, 1H; Rh−C*H*Me), 2.16 (m, 4H; CH_2*exo* cod), 2.14 (s, 6H; *p*-$Me$$C_6H_4$), 1.45 (m, 2H) and 1.32 (m, 2H; CH_2*endo* cod), 1.47 (s, 1H) and 1.11 (s, 1H; NH), 1.17 (s, 9H) and 1.16 (s, 9H; *t*Bu), 0.99 ppm (d, 3H, J(H,H) = 7.0 Hz; Rh−CHMe); ^{13}C{^{1}H} NMR (CD_2Cl_2, −50 °C): δ = 181.4 (d, ^2J(C,Rh) = 1 Hz; CO_2Me); 153.5, 153.4, 129.6, 129.5, 129.4, 129.3, 127.6, 127.4, 123.7, 123.5, 122.5 and 121.9 (*p*-MeC_6H_4), 76.5 (d, J(C,Rh) = 7 Hz), 76.3 (d, J(C,Rh) = 6 Hz) and 74.5 (m, 2C; =CH cod), 57.9 ($C(CH_3)_3$), 51.4 (CO_2Me), 31.6, 31.5, 29.7 and 29.6 (CH_2 cod), 29.8 and 29.6 (C(CH_3)$_3$), 23.6 (d, ^1J(C,Rh) = 24 Hz, Rh−C*H*Me), 21.1 (Rh−CHMe), 20.8 ppm (*p*-$Me$$C_6H_4$); IR (toluene): ν = 2210 (s), 2185 cm^{-1} (s; CN); MS: *m*/*z* (%): 814 (10) [M^+]; elemental analysis calcd (%) for $C_{36}H_{53}N_4ClO_2Rh_2$ (815.1): C 53.05, H 6.55, N 6.87; found: C 53.35, H 6.85, N 6.69.

[(cod)Rh(μ-NH{*p*-tolyl})$_2$RhCl(η¹-CH_2CO_2Me)(CN*t*Bu)$_2$] (6): Neat methyl chloroacetate (14.7 μL, 0.17 mmol) was added to a suspension of **4** (120.0 mg, 0.17 mmol) in toluene (8 mL) in the dark. After 30 min the resulting yellow solution was concentrated to about 2 mL and carefully layered with hexane (20 mL) to produce yellow microcrystals overnight. The solution was decanted and the solid washed with hexane (2×5 mL) and vacuum-dried (113.8 mg, 82 %). ^{1}H NMR ([D$_8$]toluene, −70 °C): δ = 8.91 (δA, 2H), 6.89 (δB, J(A,B) = 8.3 Hz, 2H) and 6.74 (δA, 2H), 6.66 (δB, J(A,B) = 6.7 Hz, 2H; *p*-MeC_6H_4), 3.89 (m, 2H) and 3.65 (m, 2H; = CH cod), 3.41 (s, 3H; CO_2Me), 2.77 (s, 2H; NH), 2.65 (brs, 2H; Rh−CH_2), 2.37 (m, 4H; CH_2*exo* cod), 2.13 (s, 6H; *p*-$Me$$C_6H_4$), 1.46 (s, 4H; CH_2*endo* cod), 0.71 ppm (s, 18H; *t*Bu); ^{13}C{^{1}H} NMR ([D$_8$]toluene, −70 °C): δ = 180.6 (s; CO_2Me), 153.3 (Ci), 129.8 (C*p*), 129.6 and 127.7 (C*m*), 123.3 and 121.8 (C*o*), 76.3 (d, J(C,Rh) = 14 Hz) and 74.6 (d, J-(C,Rh) = 13 Hz; =CH cod), 58.1 ($C(CH_3)_3$), 51.9 (CO_2Me), 31.5 and 29.6 (CH_2 cod), 29.7 (C(CH_3)$_3$), 21.1 (*p*-$Me$$C_6H_4$), 11.7 ppm (d, ^1J(C,Rh) = 23 Hz; Rh−CH_2); IR (toluene): ν = 2210 (s), 2185 cm^{-1} (s; CN); MS: *m*/*z* (%): 800 (35) [M^+]; elemental analysis calcd (%) or $C_{35}H_{51}N_4ClO_2Rh_2$ (801.1): C 52.48, H 6.42, N 6.99; found: C 52.53, H 6.21, N 7.12.

[(CN*t*Bu)$_2$(η¹-CH_2CO_2Me)Rh(μ-NH{*p*-tolyl})$_2$(μ-Cl)Rh(η¹-CH(Me)CO_2Me)(CN*t*Bu)$_2$]Cl ([7]Cl): CN*t*Bu (20.8 μL, 0.18 mmol), and 10 min later (−)-(*S*)-2-methylchloropropionate (100 μL, 0.71 mmol) were added to a solution of complex **6** (75.3 mg, 0.09 mmol) in toluene (10 mL). This solution was stirred for 24 h to give a suspension, which was concentrated to about 3 mL. Diethyl ether (10 mL) was then added to complete the precipitation of a white solid. The solid was filtered off, washed with diethyl ether (2×5 mL) and vacuum-dried (78.4 mg, 85 %). ^{1}H NMR ($CDCl_3$, 25 °C): δ = 7.60 (d, J(H,H) = 7 Hz, 4H) and 6.96 (m, 4H; *p*-MeC_6H_4), 3.54 (s, 3H) and 3.42 (s, 3H; CO_2Me), 3.06 (m, 1H; Rh-C*H*Me), 2.84 (s, 1H) and 2.71 (s, 1H; NH), 2.30 (d, ^3J(H,Rh) = 3.4 Hz, 2H; Rh−CH_2), 2.203 (s, 3H) and 2.198 (s, 3H; *p*-$Me$$C_6H_4$), 1.25 (s, 18H), 1.18 (s, 9H) and 1.13 (s, 9H; *t*Bu), 1.03 ppm (dd, 3H, ^3J(H,H) = 6.9, ^3J(H,Rh) = 2.4 Hz; Rh−CHMe); ^{13}C{^{1}H} NMR ($CDCl_3$, 25 °C): δ = 179.6 and 178.7 (CO_2Me), 153.8 and 153.7 (Ci), 132.8 and 132.7 (C*p*), 128.9 and 128.7 (C*m*), 122.1 and 121.9 (C*o*), 58.6 ($C(CH_3)_3$), 51.4 and 51.2 (CO_2Me), 29.72, 29.66, 29.64 and 29.61 (C(CH_3)$_3$), 24.4 (d, J(C,Rh) = 25 Hz; Rh−C*H*Me), 21.5 (Rh−CHMe), 20.6 (*p*-$Me$$C_6H_4$); 11.3 ppm (d, J(C,Rh) = 25 Hz; Rh−CH_2); IR (CH_2Cl_2): ν = 2220 (s), 2201 cm^{-1} (s; CN); MS: *m*/*z* (%): 945 (100) [M^+]; Λ_M (5×10^{-4} M in acetone) = 107.9 S mol^{-1} cm^{-1}; elemental analysis calcd (%) for $C_{41}H_{64}N_6Cl_2O_4Rh_2\cdot C_7H_8$ (1073.9): C 53.69, H 6.75, N 7.82; found: C 54.10, H 6.80, N 7.78.

Compound [7]Tf: MeTf (8.8 μL, 0.08 mmol) was added to a solution of [**7**]Cl (78.5 mg, 0.08 mmol) in acetone (3 mL). After 2 h, the solution was carefully layered with diethyl ether (10 mL) to render, after 2 d in the

dark, white crystals suitable for X-ray diffraction studies. The mother liquor was decanted, and the crystals were dried under vacuum (70.0 mg, 80%). Elemental analysis calcd (%) for $C_{42}H_{64}N_6ClF_3O_7SRh_2$: C 46.06, H 5.89, N 7.67, S 2.93; found: C 45.89, H 6.01, N 7.83, S 3.20.

[{RhCl(μ-NH{*p*-tolyl})(CN*t*Bu)$_2$}$_2$(μ-CH$_2$)] (8): Compound **1** (100.0 mg, 0.13 mmol) was dissolved in dichloromethane (7 mL) in the dark. After 30 min of reaction, the orange solution was concentrated to 2 mL and layered with pentane (15 mL) to render orange microcrystals after 3 d. The crystals were filtered, washed with pentane (2×5 mL), and vacuum-dried (104.5 mg, 90%). ^{1}H NMR ($CDCl_3$, 25°C): δ = 7.23 (δA, 2H) and 6.96 (δB, J(A,B) = 8.2 Hz, 2H; *p*-Me$C_6H_4^A$), 7.14 (δA, 2H) and 6.81 (δB, J(A,B) = 8.2 Hz, 2H; *p*-Me$C_6H_4^B$), 3.84 (m, 1H) and 3.02 (s, 1H; μ-CH_2), 2.47 (s, 1H) and 1.64 (s, 1H; NH), 2.17 (s, 3H; *p*-*Me*$C_6H_4^A$), 2.15 (s, 3H; *p*-*Me*$C_6H_4^B$), 1.49 (s, 18H) and 1.26 ppm (s, 18H; *t*Bu); ^{13}C{^{1}H} NMR ($CDCl_3$, 25°C): δ = 156.0 and 148.7 (Ci), 135.7 (m; *C*NC(CH$_3$)$_3$), 130.3 and 128.5 (C*p*), 128.6 and 128.3 (C*m*), 123.9 and 121.7 (C*o*), 57.8 and 57.5 ($C(CH_3)_3$), 30.7 and 29.9 (C(CH_3)$_3$), 29.8 (t, J(C,Rh) = 23 Hz; μ-CH_2), 20.9 and 20.3 ppm (*p*-*Me*C_6H_4); IR (CH_2Cl_2): ν = 2199 (s), 2176 cm^{-1} (s; CN); MS: *m*/*z* (%): 834 (15) [M^+], 799 (100) [M^+−Cl]; elemental analysis calcd (%) for $C_{35}H_{54}N_6Cl_2Rh_2{\cdot}2H_2O$ (871.6): C 48.23, H 6.71, N 9.64; found: C 47.98, H 6.68, N 9.49.

[(cod)ClRh(μ-CH$_2$)(μ-NH{*p*-tolyl})$_2$RhCl(CN*t*Bu)$_2$] (9): Compound **4** (100.0 mg, 0.14 mmol) was dissolved in dichloromethane (7 mL) and the solution was maintained in the dark for 1 d. The resulting orange solution was concentrated to 2 mL and then layered with pentane (15 mL) to render orange microcrystals after 4 d. The crystals were filtered, washed with pentane (2×5 mL), and vacuum-dried to yield 94.0 mg (80%). ^{1}H NMR ([D$_6$]acetone, 25°C): δ = 7.31 (δA, 4H), 6.97 (δB, J(A,B) = 8.1 Hz, 4H; *p*-MeC_6H_4), 5.47 (t, ^2J(H,Rh) = 1.2 Hz, 2H; μ-CH_2), 4.16 (m, 4H; =CH cod), 3.04 (s, 2H; NH), 2.58 (m, 4H; CH_2*exo* cod), 2.19 (s, 6H; *p*-*Me*C_6H_4), 1.94 (m, 2H) and 1.75 (m, 2H; CH_2*endo* cod), 1.51 ppm (s, 18H; *t*Bu); ^{13}C{^{1}H} NMR ($CDCl_3$, 25°C): δ = 150.4 (Ci), 131.2 (C*p*), 128.6 (C*m*), 121.9 (C*o*), 103.5 (d, J(C,Rh) = 7 Hz) and 101.6 (d, (C,Rh) = 7 Hz; =CH cod), 58.1 ($C(CH_3)_3$), 45.5 (t, J(C,Rh) = 19 Hz; μ-CH_2), 30.3 (C(CH_3)$_3$), 29.3 and 28.3 (CH_2 cod), 20.7 ppm (*p*-*Me*C_6H_4); IR (CH_2Cl_2): ν = 2206 (s), 2181 cm^{-1} (s; CN); MS: *m*/*z* (%): 777 (15) [M^+], 741 (100) [M^+−Cl]; elemental analysis calcd (%) for $C_{33}H_{48}N_4Cl_2Rh_2{\cdot}2H_2O$ (813.6): C 48.72, H 6.44, N 6.89; found: C 49.15, H 6.25, N 6.95.

[(CN*t*Bu)$_2$(η^1-CH$_2$Cl)Rh(μ-NH{*p*-tolyl})$_2$(μ-Cl)Rh(η^1-CH(Me)CO$_2$Me)-(CN*t*Bu)$_2$]Cl ([10]Cl): *tert*-Butylisocyanide (27.2 μL, 0.24 mmol) was added to a solution of **5** (100 mg, 0.12 mmol) in dichloromethane. After stirring for 30 min the solution was concentrated to 2 mL and then layered with diethyl ether (15 mL) to render yellow microcrystals in 4 d. The solution was decanted and the solid was washed with cold diethyl ether and vacuum-dried (99.0 mg, 86%). ^{1}H NMR ([D$_6$]acetone, 25°C): δ = 7.77 (δA, 2H) and 7.04 (δB, J(A,B) = 8.4 Hz, 2H; *p*-Me$C_6H_4^A$), 7.67 (δA, 2H) and 7.02 (δB, J(A,B) = 8.4 Hz, 2H; *p*-Me$C_6H_4^B$), 5.02 (δA, ^2J(H,Rh) = 2.7 Hz, 1H) and 4.95 (δB, J(A,B) = 8.4, ^2J(H,Rh) = 3.0 Hz, 1H; Rh−CH_2), 4.75(s, 1H) and 4.26 (s, 1H; NH), 4.52 (m, 1H; Rh−C*H*Me), 3.92 (s, 3H; CO_2*Me*), 2.24 (s, 6H; *p*-*Me*C_6H_4), 1.34 (s, 18H) and 1.24 (s, 18H; *t*Bu), 1.00 ppm (dd, J(H,H) = 6.6, ^3J(H,Rh) = 1.8 Hz, 3H; Rh−CH*Me*); ^{13}C{^{1}H} NMR ($CDCl_3$, 25°C): δ = 180.1 (CO_2Me), 154.1 and 154.0 (Ci), 132.6 and 132.5 (C*p*), 129.0 and 128.8 (C*m*), 122.2 and 122.0 (C*o*), 58.7 ($C(CH_3)_3$), 51.4 (CO_2*Me*), 37.5 (d, J(C,Rh) = 30 Hz; Rh−CH_2Cl), 29.78, 29.74, 29.64 and 29.59 (C(CH_3)$_3$), 24.1 (d, J(C,Rh) = 25 Hz, Rh−*C*HMe), 21.7 (Rh−CH*Me*), 20.67 and 20.64 ppm (*p*-*Me*C_6H_4); IR (CH_2Cl_2): ν = 2220 (s), 2201 cm^{-1} (s; CN); MS: *m*/*z* (%): 921 (100) [M^+]; Λ_M (5×10^{-4} M in acetone) = 75.1 S mol^{-1} cm^{-1}; elemental analysis calcd (%) for $C_{39}H_{61}N_6Cl_3O_2Rh_2$ (958.1): C 48.89, H 6.42, N 8.77; found: C 48.99, H 6.73, N 8.37.

[{Rh(μ-NH{*p*-tolyl})(η^1-CH$_2$CH(CH$_3$)CH$_2$CH$_3$)(CN*t*Bu)$_2$}$_2$(μ-Br)]Br ([11]Br): (+)-(*S*)-BrCH$_2$CH(CH$_3$)CH$_2$CH$_3$ (25.2 μL, 0.28 mmol) was added to a suspension of **1** (100.0 mg, 0.13 mmol) in diethyl ether (15 mL) at room temperature. After stirring for 2 h, the resulting suspension was left in the refrigerator for 2 d to render a white microcrystalline solid, which was filtered off, washed with diethyl ether (2×5 mL), and vacuum-dried (105.3 mg, 75%). ^{1}H NMR ($CDCl_3$, 25°C): δ = 7.50 (br s, 4H) and 6.98 (d, J(H,H) = 8.2 Hz, 4H; *p*-MeC_6H_4), 2.26 (s, 6H; *p*-*Me*C_6H_4), 2.18 (m, 2H) and 1.90 (m, 2H; Rh−CH_2), 1.69 (br s, 2H; NH), 1.41 (br s, 2H; CH), 1.30 (m, 4H; CH_2), 1.25 (s, 18H) and 1.23 (s, 18H; *t*Bu), 0.92 (t, 6H, J(H,H) = 7.2 Hz; CH_3), 0.87 ppm (d, 6H, J(H,H) = 6.1 Hz; CH_3); ^{13}C{^{1}H} NMR ($CDCl_3$, 25°C): δ = 154.3 (Ci), 132.1 (C*p*), 129.0 (C*m*), 121.6 (C*o*), 58.2 and 58.1 ($C(CH_3)_3$), 40.7 (CH_2), 38.4 (d, J(C,Rh) = 24 Hz; Rh−CH_2), 31.4 (CH), 29.76 and 29.70 (C(CH_3)$_3$), 21.8 (CH_3), 20.6 (*p*-*Me*C_6H_4), 12.1 ppm (CH_3); IR (CH_2Cl_2): ν = 2210 (s), 2189 cm^{-1} (s; CN); MS: *m*/*z* (%): 974 (100) [M^+]; Λ_M (3×10^{-4} M in acetone) = 108.3 S mol^{-1} cm^{-1}; [α] = 24.4 (c = 0.47 mg 100 mL^{-1}, $CHCl_3$, 23.9°C); elemental analysis calcd (%) for $C_{44}H_{74}N_6Br_2Rh_2$ (1052.7): C 50.20, H 7.08, N 7.98; found: C 50.00, H 7.28, N 7.64.

[{Rh(μ-NH{*p*-tolyl})(η^1-CH$_2$CH(CH$_3$)CH$_2$CH$_3$)(CN*t*Bu)$_2$}$_2$(μ-I)]I ([12]I): **[12]I** was prepared as described for complex [**11**]Br, but using toluene (7 mL) instead of diethyl ether and starting from **1** (100.0 mg, 0.13 mmol) and (+)-(*S*)-ICH$_2$-CH(CH$_3$)CH$_2$CH$_3$ (35.5 μL, 0.28 mmol)to yield: 105.3 mg (70%. ^{1}H NMR ($CDCl_3$, 25°C): δ = 7.45 (d, J(H,H) = 6.8 Hz, 4H) and 6.92 (d, J(H,H) = 8.0 Hz, 4H; *p*-MeC_6H_4), 2.20 (s, 6H; *p*-*Me*C_6H_4), 2.18 (m, 2H) and 1.95 (m, 2H; Rh−CH_2), 1.53 (br s, 2H; NH), 1.35 (m, 2H; CH_2), 1.24 (s, 18H) and 1.22 (s, 18H; *t*Bu), 1.16 (m, 2H; CH), 0.87 (t, 6H, J(H,H) = 8.0 Hz; CH_3), 0.84 ppm (d, 6H, J(H,H)

Table 5. Selected crystal, measurement, and refinement data for compounds [**3**]Cl-$C_s{\cdot}H_2O$, **5**, [**7**]Tf, and [**12**]I.

	[**3**]Cl-$C_s{\cdot}H_2O$	**5**	[**7**]Tf	[**12**]I
formula	$C_{42}H_{68}Cl_2N_6O_5Rh_2$	$C_{36}H_{53}ClN_4O_2Rh_2$	$C_{42}H_{62}ClF_3N_6\ O_7Rh_2S$	$C_{51}H_{80}I_2N_6O_2\ Rh_2$
formula weight	1013.74	815.09	1093.31	1278.91
color	yellow	yellow	colorless	pale yellow
crystal system	tetragonal	triclinic	monoclinic	triclinic
space group	*I*4/*m*	*P*1	$P2_1$	*P*1
a [Å]	29.1563(17)	11.6239(11)	12.279(2)	14.1638(8)
b [Å]	29.1563(17)	12.1021(14)	13.877(2)	14.8744(9)
c [Å]	13.9481(13)	15.1226(18)	15.478(3)	14.9457(9)
α [°]	90	82.056(9)	90	76.472(1)
β [°]	90	88.538(8)	106.523(3)	74.689(1)
γ [°]	90	62.700(8)	90	76.985(1)
V [Å^3]	11857.1(15)	1870.5(4)	2528.6(8)	2907.5(3)
Z	8	2	2	2
F(000)	4208	840	1124	1300
ρ_{calcd} [g cm^{-3}]	1.136	1.447	1.436	1.461
μ [mm^{-1}]	0.684	0.989	0.808	1.669
crystal size [mm]	0.38×0.22×0.21	0.50×0.32×0.26	0.22×0.13×0.05	0.35×0.13×0.07
T [K]	173(2)	150(2)	293(2)	100(2)
θ limits [°]	1.62 to 26.00	1.91 to 25.99	2.27 to 25.20	1.43 to 27.00
collected reflns.	12124	10800	18779	34521
unique reflns. (R_{int})	6080 (0.0400)	7245 (0.0181)	9081 (0.0484)	24590 (0.0210)
reflns. with $I>2\sigma(I)$	4916	6309	7783	21482
parameters/restraints	296/30	464/6	579/31	1147/17
R_1 (on F, $I>2\sigma(I)$)	0.0407	0.0333	0.0487	0.0394
wR_2 (on F^2, all data)	0.1098	0.0868	0.1076	0.0966
max/min $\Delta\rho$ [e Å^{-3}]	0.914/−0.531	0.635/−0.457	0.629/−0.511	1.064/−0.864

= 6.5 Hz; CH_3); $^{13}C\{^1H\}$ NMR ($CDCl_3$, 25 °C): δ = 154.0 (Ci), 132.2 (C*p*), 129.0 (C*m*), 122.1 (C*o*), 58.2 and 58.1 ($C(CH_3)_3$), 43.2 (d, J(C,Rh) = 24 Hz; Rh–CH_2), 40.8 (CH_2), 31.7 (CH), 29.86 and 29.80 ($C(CH_3)_3$), 21.9 (CH_3), 20.6 (*p*-*Me*C_6H_4), 12.2 ppm (CH_3); IR (toluene): ν = 2207 (s), 2183 cm^{-1} (s; CN); MS: *m*/*z* (%): 1020 (100) [M^+]; Λ_M (3×10^{-4} M in acetone) = $108.3\times S\,mol^{-1}\,cm^{-1}$; [$\alpha$] = 25.8 ($c$ = 0.47 mg 100 mL^{-1}, $CHCl_3$, 24.1 °C); elemental analysis calcd (%) for $C_{44}H_{74}N_6I_2Rh_2.C_7H_8$ (1238.8): C 49.45, H 6.67, N 6.78; found: C 49.71, H 6.45, N 6.56.

X-ray diffraction studies on [3]Cl-C_s·H_2O, 5, [7]Tf and [12]I: Intensity measurements were collected with Siemens–Stoe AED-2 ([**3**]Cl-C_s·H_2O), Siemens P4 (**5**) and Bruker Smart Apex ([**7**]Tf and [**12**]I) diffractometers, with graphite-monochromated Mo Kα radiation. A semi-empirical absorption correction was applied to each data set, with the psi scan[24] ([**3**]Cl-C_s·H_2O and **5**) or multi-scan[25] ([**7**]Tf and [**12**]I) methods. Selected crystallographic data can be found in Table 5. The structures were solved by the Patterson method and refined by the full-matrix least-squares method, with the program SHELX97[26] in the WINGX[27] package.

CCDC-612663, -612664, -612665, and -612666 contain the supplementary crystallographic data for this paper. These data can be obtained free of charge from The Cambridge Crystallographic Data Centre via www.ccdc.cam.ac.uk/data_request/cif.

Acknowledgements

The generous financial support from MEC/FEDER (Project CTQ2005-06807/BQU) and DGA (Research group E70) is gratefully acknowledged. S.J. thanks DGA (Diputación General de Aragón) for a fellowship.

[1] a) M. Huser, M.-T. Youinou, J. A. Osborn, *Angew. Chem.* **1989**, *101*, 1427; *Angew. Chem. Int. Ed. Engl.* **1989**, *28*, 1386; b) W. A. Herrmann, G. Brossmer, T. Priermeier, K. Ofele, *J. Organomet. Chem.* **1994**, *481*, 97; c) V. V. Grushin, H. Alper, *Chem. Rev.* **1994**, *94*, 1047.

[2] a) D. Milstein, *Acc. Chem. Res.* **1988**, *21*, 428; b) J. P. Collman, L. S. Hegedus, J. R. Norton, R. G. Finke, *Principles and Applications of Organotransition Metal Chemistry*, 2nd ed., University Science Books, Mill Valley CA, **1987**.

[3] L. M. Rendina, R. Puddephatt, *Chem. Rev.* **1997**, *97*, 1735.

[4] C. M. Thomas, G. Süss-Fink, *Coord. Chem. Rev.* **2003**, *243*, 125.

[5] A. Haynes, P. M. Maitlis, G. E. Morris, G. J. Sunley, H. Adams, P. W. Badger, C. M. Bowers, D. B. Cook, P. I. P. Elliot, T. Ghaffar, H. Green, T. R. Griffin, M. Paynes, J. M. Pearson, M. J. Taylor, P. W. Vickers, R. J. Watt, *J. Am. Chem. Soc.* **2004**, *126*, 2847.

[6] a) J. M. Fritsch, K. McNeil, *Inorg. Chem.* **2005**, *44*, 4852; b) N. Coute, J. T. Richardson, *Appl. Catal. B* **2000**, *26*, 265.

[7] a) R. B. Bedford, C. S. J. Cazin, D. Holder, *Coord. Chem. Rev.* **2004**, *248*, 2283; b) X. H. Bei, A. Hagemeyer, A. Volpe, R. Saxton, H. Turner, A. S. Guram, *J. Org. Chem.* **2004**, *69*, 8626; c) A. Zapf, M. Beller, *Chem. Eur. J.* **2001**, *7*, 2908; d) P. Machnitzki, O. Stelzer, W. S. Sheldrick, C. Landfrage, *J. Organomet. Chem.* **1998**, *554*, 207; e) P. Leoni, *Organometallics* **1993**, *12*, 2432.

[8] a) M. Crespo, C. Grande, A. Klein, M. Font-Bardía, X. Solans, *J. Organomet. Chem.* **1998**, *563*, 179; b) K. Sunkel, U. Birk, C. Robl, *Organometallics* **1994**, *13*, 1679.

[9] a) K. T. K. Chan, L. P. Spencer, J. D. Masuda, J. S. J. McCahill, P. Wei, D. W. Stephan, *Organometallics* **2004**, *23*, 381; b) T. Kawamoto, *Inorg. Chim. Acta* **2000**, *300*, 512.

[10] A. von Zelewsky, A. P. Suckling, H. Stoeckli-Evans, *Inorg. Chem.* **1993**, *32*, 4585.

[11] J. Le Bras, H. Amouri, J. Vaissermann, *J. Organomet. Chem.* **1997**, *548*, 305.

[12] a) B. C. De Pater, E. J. Zijp, H.-W. Frühauf, J. M. Ernsting, C. J. Elsevier, K. Vrieze, *Organometallics* **2004**, *23*, 269; b) E. Teuma, F. Malbosc, M. Etienne, J.-C. Daran, P. Kalck, *J. Organomet. Chem.* **2004**, *689*, 1763; c) H. F. Haarman, J. M. Ernsting, M. Kranenburg, H. Kooijman, N. Vedman, A. L. Spek, P. W. N. M. Van Leeuwen, K. Vrieze, *Organometallics* **1997**, *16*, 887.

[13] T. Yoshida, T. Ueda, T. Adachi, K. Yamamoto, T. Higuchi, *J. Chem. Soc. Chem. Commun.* **1985**, 1137.

[14] a) T. S. Lobana, K. Isobe, H. Kitayama, T. Nishioka, I. Kinoshita, *Angew. Chem.* **2004**, *116*, 215; *Angew. Chem. Int. Ed.* **2004**, *43*, 213; b) T. S. Lobana, K. Isobe, H. Kitayama, T. Nishioka, M. Doe, I. Kinoshita, *Organometallics* **2004**, *23*, 5347.

[15] T. B. Marder, W. C. Fultz, J. C. Calabrese, R. L. Harlow, D. Milstein, *J. Chem. Soc. Chem. Commun.* **1987**, 1543.

[16] a) F. Barrios-Landeros, J. F. Hartwig, *J. Am. Chem. Soc.* **2005**, *127*, 6944; b) P. Espinet, A. Echavarren, *Angew. Chem.* **2004**, *116*, 4808; *Angew. Chem. Int. Ed.* **2004**, *43*, 4704; c) A. K. de K. Lewis, S. Caddick, F. G. N. Cloke, N. C. Billingham, P. B. Hitchcock, J. Leonard, *J. Am. Chem. Soc.* **2003**, *125*, 10066; d) A. H. Roy, J. F. Hartwig, *J. Am. Chem. Soc.* **2003**, *125*, 13944; e) L. M. Alcázar-Román, J. F. Hartwig, *J. Am. Chem. Soc.* **2001**, *123*, 12905.

[17] a) C. Tejel, M. A. Ciriano, L. A. Oro, A. Tiripicchio, F. Ugozzoli, *Organometallics* **2001**, *20*, 1676; b) C. Tejel, M. A. Ciriano, J. A. López, F. J. Lahoz, L. A. Oro, *Organometallics* **2000**, *19*, 4968; c) L. A. Oro, M. A. Ciriano, C. Tejel, *Pure Appl. Chem.* **1998**, *70*, 779; d) C. Tejel, M. A. Ciriano, L. A. Oro, A. Tiripicchio, F. Ugozzoli, *Organometallics* **1994**, *13*, 4153.

[18] a) C. Tejel, M. A. Ciriano, J. A. López, F. J. Lahoz, L. A. Oro, *Organometallics* **2000**, *19*, 4977; b) C. Tejel, M. A. Ciriano, J. A. López, F. J. Lahoz, L. A. Oro, *Organometallics* **1998**, *17*, 1449.

[19] R. Dorta, L. J. W. Shimon, H. Rozenberg, D. Milstein, *Eur. J. Inorg. Chem.* **2002**, 1827.

[20] a) C. Tejel, M. A. Ciriano, M. Bordonaba, J. A. López, F. J. Lahoz, L. A. Oro, *Inorg. Chem.* **2002**, *41*, 2348; b) C. Tejel, M. A. Ciriano, M. Bordonaba, J. A. López, F. J. Lahoz, L. A. Oro, *Chem. Eur. J.* **2002**, *8*, 3128.

[21] a) J. A. Labinger, J. A. Osborn, *Inorg. Chem.* **1980**, *19*, 3230; b) J. A. Labinger, J. A. Osborn, N. J. Coville, *Inorg. Chem.* **1980**, *19*, 3236.

[22] M. Retboll, Y. Ishii, M. Hidai, *Chem. Lett.* **1998**, 1217.

[23] H. Matsuzaka, T. Kamura, K. Ariga, Y. Watanabe, T. Okubo, T. Ishii, M. Yamashita, M. Kondo, S. Kitagawa, *Organometallics* **2000**, *19*, 216.

[24] A. C. T. North, D. C. Phillips, F. S. Mathews, *Acta Crystallogr. Sect. A* **1968**, *24*, 351.

[25] G. M. Sheldrick, *SADABS*, Bruker AXS, Madison, WI, **1997**.

[26] G. M. Sheldrick, *SHELXL-97: Program for Crystal Structure Refinement*, University of Göttingen, Göttingen (Germany), **1997**.

[27] L. J. Farrugia, *J. Appl. Crystallogr.* **1999**, *32*, 837.

Received: July 7, 2006
Published online: November 29, 2006

